Resonant flux motion and I-V characteristics in frustrated Josephson junctions

N. Stefanakis
CNRS-CRTBT, 25 Avenue des Martyrs, BP 166-38042, Grenoble cédex 9, France
(Received 13 February 2002; revised manuscript received 23 July 2002; published 31 December 2002)

We describe the dynamics of fluxons moving in a frustrated Josephson junction with *p*-, *d*-, and *f*-wave symmetry and calculate the I-V characteristics. The behavior of fluxons is quite distinct in the long- and short-length junction limits. For long junctions the intrinsic flux is bound at the center and the moving integer fluxon or antifluxon interacts with it only when it approaches the junction's center. For small junctions the intrinsic flux can move as a bunched-type fluxon introducing additional steps in the I-V characteristics. A possible realization in quantum computation is presented.

DOI: 10.1103/PhysRevB.66.214524 PACS number(s): 74.50.+r, 74.20.Rp, 74.60.Jg, 85.25.Hv

I. INTRODUCTION

The determination of the order parameter symmetry in high-T_c superconductors is a problem which has not yet been completely solved.[1–8] The Josephson effect provides a phase-sensitive mechanism to study the pairing symmetry of unconventional superconductors. In Josephson junctions involving unconventional superconductors, the sign change of the order parameter with angle measured from the x axis in the ab plane introduces an intrinsic phase shift of π in the Josephson current phase relation or alternatively a negative Josephson critical current. The effect of shifting the phase by π is equivalent to shifting the critical current versus the magnetic flux pattern in a superconducting quantum interference device (SQUID) that contains a π junction (called a frustrated junction) by $\Phi_0/2$, where $\Phi_0=h/2e$ is the flux quantum.[2]

The presence of spontaneous or trapped flux is a general property of systems where a sign change of the pair potential occurs in orthogonal directions in k space. Its existence has been predicted for example in ruthenates[9] where the pairing state is triplet as indicated in Knight shift measurements[10] and the time-reversal symmetry is broken as shown by the muon spin rotation (μSR) experiment[11] where the evolution of the polarization of the implanted muon in the local magnetic environment of the superconductor gives information about the presence of a spontaneous magnetic field. Moreover, the pairing state has line nodes within the gap as indicated by specific heat measurements.[12] This spontaneous flux shows a characteristic modulation with the misorientation angle within the RuO_2 plane that can be checked by experiment.[13]

The one-dimensional Josephson junction with total reflection at the end boundaries, between *s*-wave superconductors, supports modes of the resonant propagation of fluxons.[14] In the plot of the current-voltage (I-V) characteristics these modes appear as near-constant voltage branches known as zero-field steps (ZFS's).[15–17] They occur in the absence of any external field. The ZFS's appear at integer multiple of $V_1=\Phi_0 c_S/l$, where c_S is the velocity of the electromagnetic waves in the junction and l is the junction length. The moving fluxon is accompanied by a voltage pulse which can be detected at the junction's edges.

When the contact between a 0 and π junction, which contains an intrinsic half-fluxon, is current biased the half-fluxon becomes unstable for certain values of the external current with respect to transforming into an anti-half-fluxon and emitting an integer fluxon.[18] Also when a 0-π-0 junction, which contains two half vortices, is current biased, for certain critical current, a transition occurs between the two degenerate fluxon configurations and a voltage pulse is generated.[19]

In this paper we study the dynamic properties of fluxons and calculate the I-V characteristics in frustrated junctions with B_{1g}, E_u, and $B_{1g}\times E_u$ pairing symmetry. The last two are candidates pairing states for ruthenates.[9] The nodeless *p*-wave order parameter with E_u symmetry has been proposed by Rice and Sigrist[20] while the $B_{1g}\times E_u$ has been proposed by Hasegawa *et al.*[21] In junctions involving unconventional superconductors the behavior of fluxons is typically different in the long- and short-length junction limits. In the long limit the fractional fluxon is confined at the center and the moving fluxon interacts with it only when it approaches the center. However, in the short limit the bound fluxon becomes able to move as a bunched-type solution with integer or half-integer magnetic flux. For the B_{1g} case the I-V pattern is shifted by a voltage that corresponds to the intrinsic phase shift. Also the frustrated Josephson junction can be considered as a way to build a quantum ''bit'' (qubit) which is the generalization of the bit of the classical computer. A readout and a preparation protocol is proposed.

The article is organized as follows. In Sec. II we develop the model and discuss the formalism. In Sec. III we present the results for the long-junction and in Sec. IV for the shorter-junction limits. In Sec. V we discuss the implementation of the qubit and finish with the conclusions.

II. CORNER JUNCTION MODEL

We consider the junction shown in Fig. 1(a) between a superconductor A with a two-component order parameter and a superconductor B with *s*-wave symmetry. The supercurrent density can be written as

$$J(\phi)=\tilde{J}_c \sin(\phi+\phi_c), \tag{1}$$

where $\tilde{J}_c$ is the Josephson critical current density, ϕ is the relative phase difference between the two superconductors,

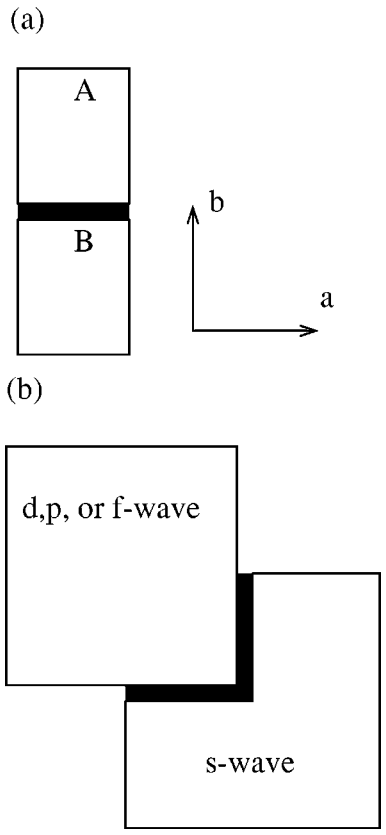

FIG. 1. (a) A single Josephson junction between superconductors *A* and *B* with a two-component order parameter. Also a small coordinate system indicating *a* and *b* crystalline directions is shown. (b) The geometry of the corner junction between a mixed-symmetry superconductor and an *s*-wave superconductor.

and ϕ_c is the intrinsic phase shift. We describe a frustrated junction of length l; i.e., the two segments have different characteristic phases, i.e., ϕ_{c1} in $0<x<l/2$ and ϕ_{c2} in $l/2<x<l$. By introducing an extra relative phase in one part of this junction, this one-dimensional junction can be mapped in the corner junction that is seen in Fig. 1(b). The characteristic phases ϕ_{c1} and ϕ_{c2} distinguish the various pairing symmetries and can be seen in Table I. For the orientation of the junction that we consider in which the *a* and *b* crystal axes are at right angles to the interface a simple calculation[5,6,13] gives $\tilde{J}_c=1$ for the pairing states that we consider.

The phase difference across the junction is then the solution of the time-dependent sine-Gordon equation

TABLE I. We present the characteristic phases ϕ_{c1} and ϕ_{c2} for the various pairing symmetries. ϕ_{c1} and ϕ_{c2} are the extra phase differences in the two edges of the corner junction due to the different orientations of the *a* axis of the crystal lattice.

Pairing state	ϕ_{c1}	ϕ_{c2}
B_{1g}	0	π
E_u	0	$-\pi/2$
$B_{1g}\times E_u$	0	$\pi/2$

$$\frac{d^2\phi}{dx^2}-\frac{d^2\phi}{dt^2}=J(\phi)+\gamma\frac{d\phi}{dt}, \tag{2}$$

with the following in-line boundary conditions:

$$\left.\frac{d\phi}{dx}\right|_{x=0,l}=\pm\frac{I}{2}, \tag{3}$$

where the time t is in units ω_0^{-1}, where $\omega_0=\sqrt{2\pi\tilde{J}_c/\Phi_0 C}$ is the Josephson plasma frequency and C is the capacitance per unit length. $\gamma=G/\omega_0 C$ is the damping constant which depends on the temperature, and G^{-1} is an effective normal resistance. The value used in the numerical calculations is $\gamma=0.01$. The length x is normalized in units of the Josephson penetration depth $\lambda_J=\sqrt{\Phi_0/2\pi\tilde{J}_c L_p}$, and L_p is the inductance per length and is given by $L_p=\mu_0 d$, where $d=2\lambda_L+t_{ox}$ is the magnetic thickness of the junction, λ_L is the London penetration depth, t_{ox} is the thickness of the insulating oxide layer, and $\mu_0=4\pi\times10^{-7}$ H/m. The velocity of the electromagnetic waves in the junction is given by $c_S=\sqrt{L_p C}$. I is the normalized inline bias current in units of $\lambda_J\tilde{J}_c$.

In a previous publication[6] we used overlap boundary conditions, where the current is uniformly distributed in space. However, in actual experiments in the *s*-wave case, the biased current in the overlap geometry may be concentrated at the edges within a length λ_J rather than distributed in space.[22] Therefore it is more appropriate to use in-line boundary conditions. However, in the case of the overlap geometry only details of the fluxon propagation are quantitatively different, e.g., the oscillations of the bound fluxons about their equilibrium position and their interaction with the moving fluxons. However, the basic physics of the problem, i.e., the shift of the voltage values, is independent of the choice of boundary conditions.

III. LONG-JUNCTION LIMIT

A fourth-order Runge-Kutta method with fixed time step $\Delta t=0.01$ was used for the integration of the equations of motion. The number of grid points is $N=1000$. We discuss first the case where the junction length is long $l=20$. We present in Fig. 2 the I-V characteristics for the first and second ZFS's that correspond to the case where one or two fluxons are moving into the junction. The pairing state is B_{1g} (a), E_u (b), and $B_{1g}\times E_u$ (c). For B_{1g} the external current cannot move the fractional fluxon (ff) which is confined at $x=0$ [see Fig. 3(b)]. However, for certain values of the bias current the ff is transformed into an fractional antifluxon (faf) and an integer fluxon (F) is emitted which is traveling to the left. The F hits the left boundary and transforms into an integer antifluxon (AF) which moves to the right. When the AF reaches the center it interacts with the faf but is not able to change its polarity and results in an faf and an AF moving to the right. The antifluxon hits the right boundary and transforms into a fluxon which moves to the center where it meets the oscillating faf and interacts with it, forming a ff, and the period is completed.

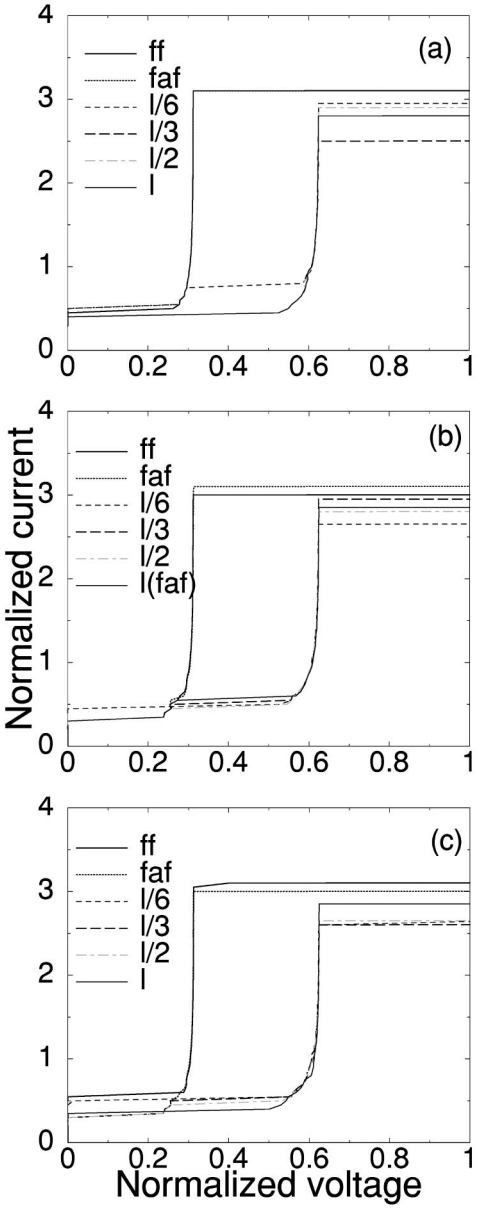

FIG. 2. Normalized current vs the normalized voltage for the in-line geometry, for the first and second ZFS's. The solutions for the first ZFS are the ff and faf corresponding to a bound fluxon or antifluxon in the junction's center. For the second ZFS the solutions are labeled by the relative distance between the fluxons l/x, where $l=20$ is the junction length, and $x=1,2,3,6$, respectively, $\gamma=0.01$. The pairing state is (a) B_{1g} wave, (b) E_u wave, and (c) $B_{1g}\times E_u$ wave.

When a faf exists at the junction center, by applying the external current it emits an AF which moves to the right and it converts itself to a ff [see Fig. 3(a)]. The AF hits the right boundary and transforms into a F which moves to the left. When the F reaches the center it interacts with the ff and results in a ff and a F moving to the left. The fluxon hits the left boundary and transforms into an antifluxon which moves to the center where it meets the oscillating ff and interacts with it, forming a faf, and the period is completed.

In the relativistic limit $c_S\approx 1$ reached at high currents a full period of motion back and forth takes time $t=2l/c_S=40$, and since the overall phase advance is 4π, the normalized voltage will be $V=\phi_t=4\pi/40=0.314$ for the first ZFS. So when the junction length is large, the ZFS's occur at the same values of the dc voltage independently of the pairing symmetry, since one full fluxon or antifluxon propagates in the junction. These values match exactly the ones for conventional *s*-wave superconductors junctions. The direction of the voltage pulse depends on the sign of the intrinsic flux and can be used for the qubit implementation.

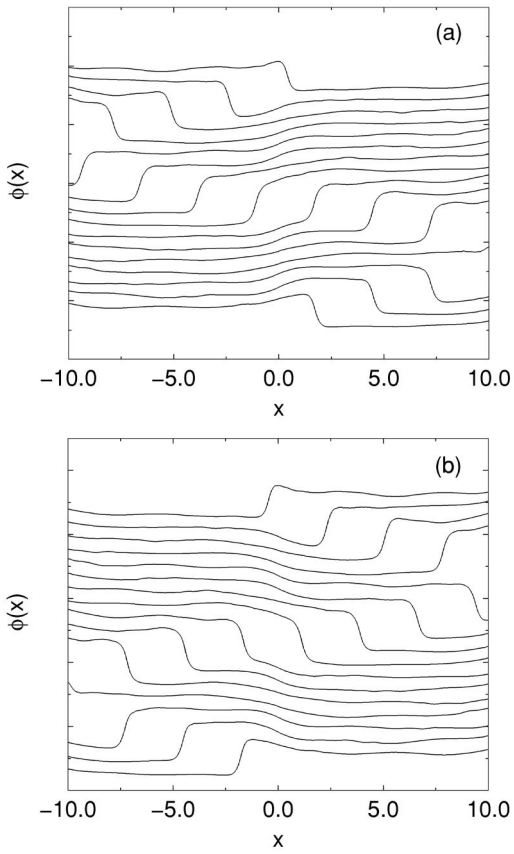

FIG. 3. Phase $\phi(x)$ vs x for the solutions in the first ZFS, at various instants, during one period separated by $\Delta\tau=2.8$. The curves are shifted by 0.5 to avoid overlapping. $l=20$, $I=1.6$, and $\gamma=0.01$: (a) ff and (b) faf. The pairing state is B_{1g} wave.

The different character of the various fluxon solutions can also be seen from the plot of the instantaneous voltage ϕ_t at the center of the junction for the various fluxon configurations. This plot is seen in Fig. 4 for the solutions regarding the first ZFS. During the time of one period three peaks appear in this plot by the time the fluxon (antifluxon) passes through the junction center. For the first ZFS the ϕ_t vs t plot can be used to probe the existence of a ff or faf at the junction center. The height of the middle peak is smaller for a bound ff at the junction center than for a bound faf. We note that for the *s*-wave case the ϕ_t vs t pulses have equal height for the forward and backward directions. The plot of ϕ_t at the edges shows two peaks at time instants which differ by half a period. The characteristic oscillations of ϕ_t between the peaks are due to the oscillation of the bound solu-

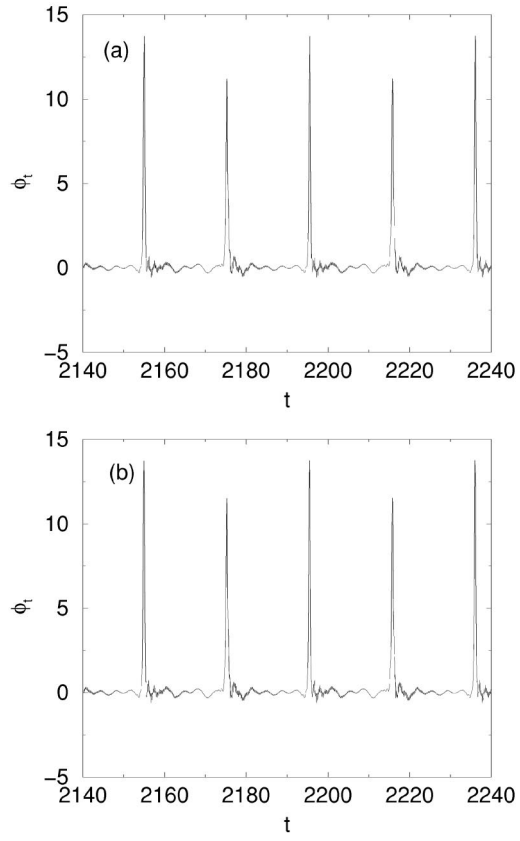

FIG. 4. Instantaneous voltage in the middle of the junction ($x=0$) vs time t, for the solutions in the first ZFS. $l=20$, $\gamma=0.01$, and $I=1.6$: (a) ff and (b) faf. The pairing state is B_{1g} wave.

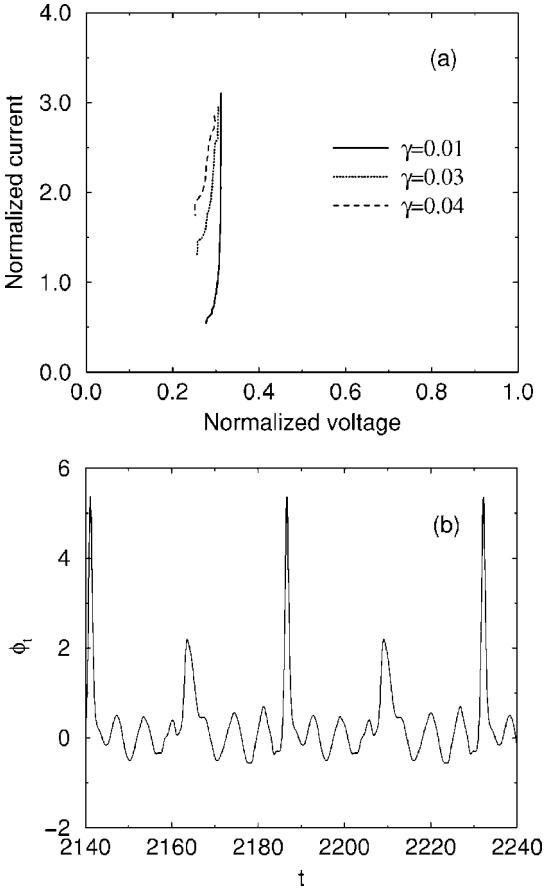

FIG. 5. (a) Normalized current vs the normalized voltage for the in-line geometry, for the ff solution, for different values of the damping constant γ. $l=20$. The pairing state is B_{1g} wave. (b) Instantaneous voltage in the middle of the junction ($x=0$) vs time t, for the solution ff, $l=20$ and $I=1.6$. The pairing state is B_{1g} wave. The damping constant is $\gamma=0.03$.

tion about the junction center. These oscillations have the same amplitude for the ff and faf cases.

For the B_{1g} case the bound fluxon and antifluxon have equal magnitudes or contain equal magnetic flux and the critical current is the same as seen in Fig. 2(a). However, for the E_u case the ff contains less flux than faf and has smaller critical current as seen in Fig. 2(b). For the $B_{1g}\times E_u$ case the ff contains more flux than faf and has greater critical current as seen in Fig. 2(c).

For the second ZFS multiple solutions exist in which two fluxons are propagating in the junction in different configurations. These solutions can be classified depending on the fluxon separation as seen in Fig. 2 and give distinct critical currents in the I-V diagram. For all the modes in the second ZFS we can estimate the value of the constant dc voltage where they occur as follows. A full period of motion back and forth takes time $T=40$, and since the overall phase advance is 8π, in the relativistic limit where $u=1$ reached at high currents, the dc voltage across the junction will be $V=0.628$. So compared to the case of conventional s-wave superconductor junctions we observe several curves for the second ZFS depending on the relative distance between the fluxons and this may be used to probe the presence of intrinsic magnetic flux.

We also considered damping effects due to the quasiparticles because the Josephson junctions made of high-T_c materials are highly damped. In the I-V curves higher damping shifts the I-V curve upwards [see Fig. 5(a)] and the fluxon reaches the critical current velocity only for currents that are very close to the critical current where the jump to the resistive branch occurs. In this case the ZFS's are not "vertical." In the plot of the instantaneous voltage at the middle of the junction versus the time [see Fig. 5(b)] the difference in height between the peaks when the F or AF interacts with the bound ff is larger for greater values of damping. The oscillations between the peaks become very large by increasing the damping and finally make the solution unstable. We believe that these solutions are more stable for small values of the damping at least for in-line boundary conditions. In the overlap case (not presented in the figure) these solutions are more stable compared to the in-line case.

IV. SHORT-LENGTH LIMIT

When the junction length is small $l=2$ the fractional fluxon or antifluxon does not remain confined at the junction's center but is able to move along the junction as a bunched-type solution. The moving fluxon configuration could have fractional flux and additional steps are introduced

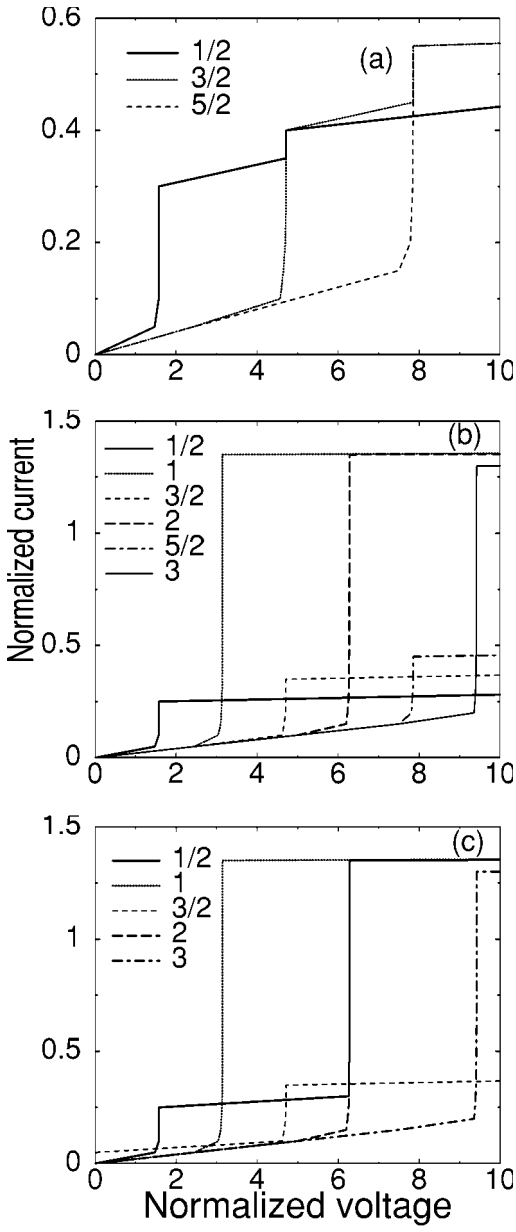

FIG. 6. Normalized current vs the normalized voltage for the in-line geometry, for a junction of length $l=2$ and $\gamma=0.01$. The different modes are labeled by the value of the normalized voltage divided by π in which they occur. The pairing state is (a) B_{1g} wave, (b) E_u wave, and (c) $B_{1g}\times E_u$ wave.

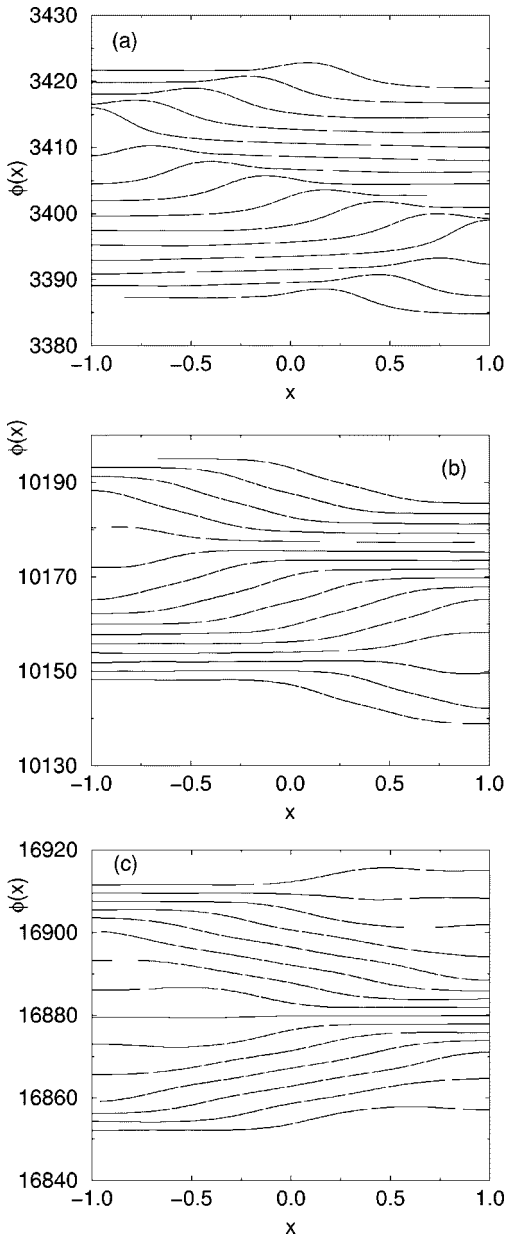

FIG. 7. Phase $\phi(x)$ vs x for the solutions in the first three ZFS's, at various instants, during one period separated by $\Delta\tau=0.2$. The pairing state is B_{1g} wave. The curves are shifted by 0.5 to avoid overlapping. $l=2$, $I=0.25$, and $\gamma=0.01$.

in the *I-V* diagram. We plot in Fig. 6 the *I-V* characteristics for the B_{1g}-, E_u-, and $(B_{1g}\times E_u)$-wave pairing states, for the small junction length $l=2$.

For the B_{1g} pairing state and the first ZFS, the moving fluxon configuration to the right is a combination of a fractional fluxon and a fractional antifluxon which contains half-integer magnetic flux [see Fig. 7(a)]. When it hits the right boundary it transforms to a configuration with opposite sign of flux which moves to the left. Then it hits the left boundary and transforms into a configuration that moves to the center and the period is completed. In the relativistic limit reached at high currents a full period of motion back and forth takes time $t=2l/c_S=4$, and since the overall phase advance is 2π, the normalized voltage will be $V=\pi/2$ as seen in Fig. 6(a) for the solution labeled as 1/2. Note that this value is half of the case where a full fluxon moves into the junction. In Fig. 8(a) we plot the ϕ_t vs t at the center of the junction where the successive peaks correspond to the passage of the fluxon combination from the junction center. The ϕ_t pulse is composed of two peaks, a positive and a negative one, corresponding to the AF and ff for the fluxon traveling in the forward direction. The pulse structures corresponding to the forward and backward directions are the same due to the symmetrical configuration of the fluxons traveling in the forward and backward directions.

It is also possible to have solutions where an integer fluxon plus a fractional fluxon is propagating into the junc-

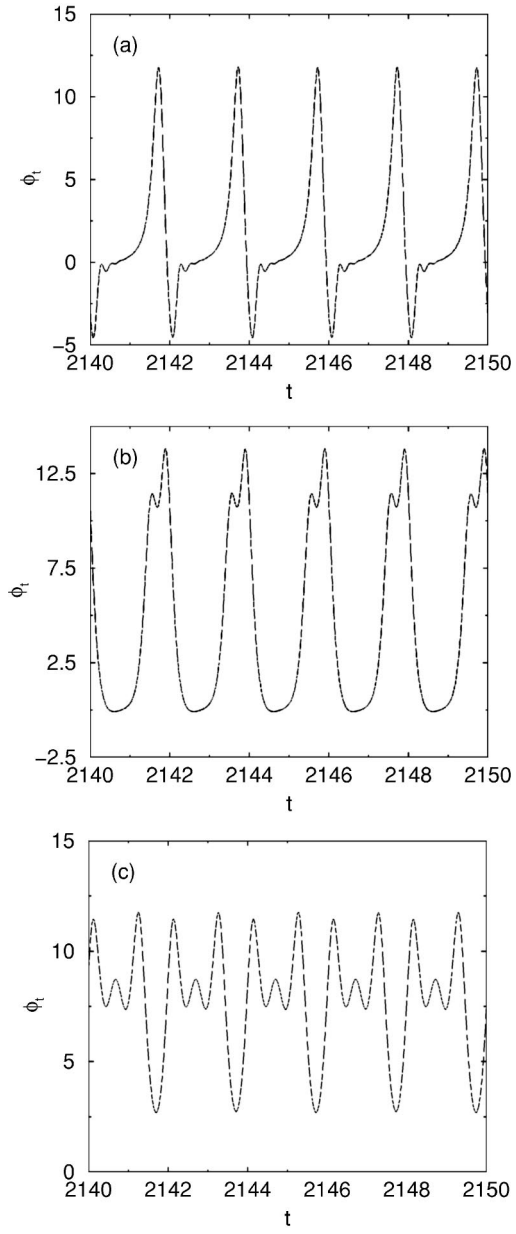

FIG. 8. Instantaneous voltage in the middle of the junction ($x=0$) vs time t, for the solutions in the first three ZFS's. The pairing state is B_{1g} wave. $l=2$, $\gamma=0.01$, and $I=0.25$.

tion [see Fig. 7(b)]. In this case the magnetic flux is equal to 1.5. In a junction of length $l=2$ the propagating fluxon accomplishes an overall phase advance of 6π in a full period $T=4$. Thus the voltage across the junction will be $V=3\pi/2$ as seen in Fig. 6(a) for the solution labeled as 3/2. In Fig. 8(b) we plot ϕ_t vs t at the center of the junction where the successive peaks correspond to the passage of the fluxon combination from the junction center. The moving fluxon or antifluxon has internal structure and therefore a double-peak structure appears in the ϕ_t vs t diagram.

Finally in Fig. 7(c) we present $\phi(x)$, for the case where two integer fluxons with a fractional fluxon in between move into the junction. This configuration contains magnetic flux equal to 2.5. Thus the dc voltage across the junction will be $V=5\pi/2$ as seen in Fig. 6(a) for the solution labeled as 5/2. In Fig. 8(c) we plot ϕ_t vs t at the center of the junction where the periodic pattern of three peaks corresponds to the passage of the integer fluxons and the half-integer fluxon from the junction's center.

So for the B_{1g} pairing state the ZFS's appear at values of the normalized voltage that are displaced by 1/2 compared to the case of s-wave superconductor junctions. This value of the voltage corresponds to the intrinsic phase shift. This is analogous to the shift of the critical current versus the magnetic flux in a corner SQUID of d-wave superconductors[2] and is expected to be confirmed by experiment.

For the E_u and $B_{1g}\times E_u$ cases, we can have additional solutions where the moving fluxon has integer flux and the voltage steps appear at values $V=n\pi$ in addition to $V=n\pi/2$ as seen in Figs. 6(b) and 6(c) for solutions labeled with integer numbers. For the B_{1g}-wave case the forward and backward configurations are symmetric and successive peak structures in the ϕ_t vs t diagram have the same form. In the E_u and $B_{1g}\times E_u$ cases, successive peaks, corresponding to the structure of the fluxon configuration that moves in the forward and backward directions, have different amplitudes, indicating that the fluxon configurations moving in the forward and backward directions have different structure.

We examined also the case where the pairing symmetry of the superconductor is $d+is$. In this case, due to the difference in the flux content of the static solutions,[5] the critical currents for the ff and faf modes of the first ZFS do not coincide.

V. QUBIT IMPLEMENTATION

Also the frustrated junction could be considered as a way to build a qubit. This idea has also been implemented using s-wave/d-wave/s-wave junction exhibiting a degenerate ground state and a double-periodic current-phase relation[23] or superconducting Josephson junction arrays.[24] Also the dynamics of a Josephson charge qubit, coupled capacitively to a current-biased Josephson junction, has been studied.[25] The two segments of the frustrated junction have characteristic energies $E(\phi)$ and $E(\phi+\pi)$, and the resulting energy exhibits a degenerate ground state. The bound ff and faf can be considered as the two quantum levels of our system.

A possible method to prepare the system in the desired ground state, i.e., ff or faf, is to apply an external magnetic field (positive or negative) and then slowly decrease it. Depending on the sign of the external field the system will go either in the ff or in the faf state. Another method is to consider the modulation of the intrinsic magnetic flux with the misorientation angle proposed in our previous work.[6]

The flux state can be determined by applying an external current. A bunched-type solution containing 0.5 (-0.5) flux is generated if the actual ground state of the system is ff (faf) which propagates into the junction to the left (right) and generates a voltage pulse which can be determined at the boundaries.

In the E_u and $B_{1g}\times E_u$ cases the actual ground state of the system is not degenerate; i.e., the ff and faf carry different flux. Moreover, the traveling fluxon caring half the flux

quantum to the left has different structure than the one traveling to the right and the ϕ_t at the ends are different for the ff and faf. In the long-length limit the presence of the ff and faf at the center can be deduced from a measurement of the ϕ_t at the edges since the direction of the moving integer flux depends on the sign of the intrinsic flux. In this case the intrinsic flux cannot escape from the junction's center.

VI. CONCLUSIONS

The fluxon dynamics in frustrated Josephson junctions with p-, d-, and f-wave pairing symmetry is different in the long- and short-junction limits. When l is large, the bound intrinsic flux remains confined at $x=0$, and the moving integer fluxon or antifluxon interacts with it only when it approaches the center. However, when the length is small the bound fluxon becomes able to move as a bunched-type solution. For d-wave junctions the I-V curves are displaced by a voltage that corresponds to the intrinsic phase shift.

The resonant fluxon motion also can be determined experimentally in one-dimensional ferromagnetic 0-π junctions where the width of the ferromagnetic oxide layer determines the region of the junction where the Josephson critical current is positive or negative.[26,27] In this case the junction contour does not have to change as in the case of a corner junction. However, the change of the junction contour was not a problem for the realization of the intrinsic fluxon in the static problem, so why should it prevent the realization of its motion?

We should also mention that when a conventional s-wave Josephson junction is biased with external magnetic field, Fiske steps (FS's) occur in the I-V characteristics with a voltage asymptote spacing just half of the ZFS's.[28] This situation is analogous to what we have reported in the present paper for frustrated junctions where the role of the external magnetic field plays the intrinsic field.

A final comment is that the frustrated junctions that we consider in this paper are realized in the (ab) plane of the unconventional superconductors due to the sign change of the order parameter. This type of junctions is different from the series array of intrinsic Josephson junctions in high-T_c supercondcutors where the Josephson effect is observed in the c axis, for instance, in $Bi_2Sr_2CaCu_2O_8$ crystals.[29]

ACKNOWLEDGMENTS

Part of this work was done at the Department of Physics, University of Crete, Greece. The author wishes to thank Dr. N. Lazarides for valuable discussions.

[1] D. J. Scalapino, Phys. Rep. **250**, 329 (1995).
[2] D. J. Van Harlingen, Rev. Mod. Phys. **67**, 515 (1995).
[3] C. C. Tsuei and J. R. Kirtley, Rev. Mod. Phys. **72**, 969 (2000).
[4] H. Hilgenkamp and J. Mannhart, Rev. Mod. Phys. **74**, 485 (2002.
[5] N. Stefanakis and N. Flytzanis, Phys. Rev. B **61**, 4270 (2000).
[6] N. Stefanakis and N. Flytzanis Phys. Rev. B **64**, 024527 (2001).
[7] N. Stefanakis, Phys. Rev. B **66**, 024514 (2002).
[8] E. Goldobin, D. Koelle, and R. Kleiner, Phys. Rev. B **66**, 100508 (2002).
[9] Y. Maeno, H. Hashimoto, K. Yoshida, S. Nishizaki, T. Fujita, G. J. Bednorz, and F. Lichtenberg, Nature (London) **372**, 532 (1994).
[10] K. Ishida, H. Mukuda, Y. Kitaoka, K. Asayama, Z. Q. Mao, Y. Mori, and Y. Maeno, Nature (London) **396**, 658 (1998).
[11] G. M. Luke, Y. Fukamoto, K. M. Kojima, M. L. Larkin, J. Merrin, B. N. Achumi, Y. J. Uemura, Y. Maeno, Z. Q. Mao, Y. Mori, H. Nakamura, and M. Sigrist, Nature (London) **394**, 558 (1998).
[12] S. Nishizaki, Y. Maeno, and Z. Mao, J. Phys. Soc. Jpn. **69**, 572 (2000).
[13] N. Stefanakis, Phys. Rev. B **65**, 064533 (2002).
[14] T. A. Fulton and R. C. Dynes, Solid State Commun. **12**, 57 (1973).
[15] J. T. Chen, T. F. Finnegan, and D. N. Langenberg, Physica (Amsterdam) **55**, 413 (1971).
[16] P. S. Lomdahl, O. H. Soerensen, and P. L. Christiansen, Phys. Rev. B **25**, 5737 (1982).
[17] I. V. Vernik, N. Lazarides, M. P. Sørensen, A. V. Ustinov, N. F. Pedersen, and V. A. Oboznov, J. Appl. Phys. **79**, 7854 (1996).
[18] A. B. Kuklov, V. S. Boyko, and J. Malinsky, Phys. Rev. B **51**, 11 965 (1995).
[19] T. Kato and M. Imada, J. Phys. Soc. Jpn. **66**, 1445 (1997).
[20] T. M. Rice and M. Sigrist, J. Phys.: Condens. Matter **7**, L643 (1995).
[21] Y. Hasegawa, K. Machida, and M. Ozaki, J. Phys. Soc. Jpn. **69**, 336 (2000).
[22] M. Scheuermann, J. R. Lhota, P. K. Kuo, and J. T. Chen, Phys. Rev. Lett. **50**, 74 (1983).
[23] L. B. Ioffe, V. B. Geshkenbein, M. V. Feigel'man, A. L. Fauchere, and G. Blatter, Nature (London) **398**, 679 (1999).
[24] D. V. Averin, Solid State Commun. **105**, 659 (1998).
[25] F. W. J. Hekking, O. Buisson, F. Balestro, and M. G. Vergniory, in *Electronic Correlations: From Meso- to Nano-physics*, edited by T. Martin, G. Montambaux, and J. Trân Thanh Vân (EDP Sciences, 2001), p. 515.
[26] O. Bourgeois, P. Gandit, J. Leseuer, A. Sulpice, X. Grison, and J. Chaussy, Eur. Phys. J. B **21**, 75 (2001).
[27] T. Kontos, M. Aprili, J. Lesueur, F. Genet, B. Stephanidis, and R. Boursier, Phys. Rev. Lett. **89**, 137007 (2002).
[28] S. N. Erné, A. Ferrigno, and R. D. Parmentier, Phys. Rev. B **27**, 5440 (1983).
[29] R. Kleiner, F. Steinmeyer, G. Kunkel, and P. Müller, Phys. Rev. Lett. **68**, 2394 (1992).